Tailoring Cooperative Emission in Molecules: Superradiance and Subradiance from First-Principles Simulations

Carlos M. Bustamante,[†] Esteban D. Gadea,[†] Tchavdar N. Todorov,[‡] and Damián A. Scherlis[*,†]

†*Departamento de Química Inorgánica, Analítica y Química Física/INQUIMAE, Facultad de Ciencias Exactas y Naturales, Universidad de Buenos Aires, Buenos Aires C1428EHA, Argentina*

‡*Centre for Quantum Materials and Technologies, School of Mathematics and Physics, Queen's University Belfast, Belfast BT7 1NN, United Kingdom*

Received December 14, 2022; E-mail: damian@qi.fcen.uba.ar

Abstract:

Cooperative optical effects provide a pathway to both the amplification (superradiance) and the supression (subradiance) of photon emission from electronically excited states. These captivating phenomena offer a rich variety of possibilities for photonic technologies aimed at electromagnetic energy manipulation, including lasers and high-speed emitting devices in the case of superradiance, or optical energy storage in that of subradiance. The employment of molecules as the building pieces in these developments requires a precise understanding of the roles of separation, orientation, spatial distribution and applied fields, which remains challenging for theory and experiments. These questions are addressed here through ab initio quantum dynamics simulations of collective emission on the basis of a novel semiclassical formalism and time-dependent DFT. By establishing the configurations leading to decoherence and how the fine-tuning of a pulse can accumulate or release optical energy in H_2 arrays, this report provides fundamental insight toward the design of real superradiant and subradiant devices.

The electromagnetic field arising from the emission of a collection of N identical entities—most often atoms, molecules, or quantum dots—can induce the coupling of their dipoles to lead to a cooperative radiative response that turns out to be qualitatively different from the behavior corresponding to the sum of the independent emitters. These correlations result in interference phenomena produced by the atomic states superposition which in turn determines the regime of photon emission. When the atomic superposition is symmetric or in phase, a fast coherent emission is induced that boosts the radiation power and accelerates the decay rate, with the intensity scaling as N^2, and the excitation lifetime reducing as $1/N$, a process that is called superradiance or superfluorescence.[1,2] Oppositely, when the atomic superposition is asymmetric or in counterphase, the light-matter interaction is decoupled and the emission rate is damped to zero, allowing for the prolongation of an excited state, an effect that is known as subradiance or limited superradiance. This is associated with the emergence of a "dark state", a term used to denote a collective non-emitting solution arising from a destructive superposition of quantum states.

These phenomena were anticipated theoretically in 1954 by Robert Dicke,[3] who developed the quantum-mechanical framework currently used to describe them. Superradiance was experimentally observed for the first time about twenty years later, in an optically pumped sample of HF gas.[4] Thereafter, it was reproduced in a variety of systems, from dilute gases to molecular arrays in the condensed phase.[5–17] The empirical evidence for subradiance, a process extremely sensitive to decoherence and therefore more elusive, is instead relatively recent and scarce.[18–21] In any case, both effects have been the subject of sustained theoretical and experimental research, for the interest that they have in the context of quantum control, electromagnetic energy storage, lasers, high speed light-emitting devices, or fast optical-based sensing, communication and information processing.[22–34]

A complete theoretical description of superradiance and subradiance requires a quantum electrodynamics treatment including the photon degrees of freedom plus the electron-photon interaction, which can be very demanding numerically even for the simulation of the smallest molecules. Simpler models based on master equations derived from the Born-Markov approximation or from the classical optical Bloch equation have proved useful in a number of situations.[2,21,35] However, these are often limited to parameterized two-level systems, inadequate for a quantitative treatment of many-electrons atoms or molecules. The same considerations apply to the so called Linblad master equations,[36,37] which involve a phenomenological coupling between the electrons and the field, typically a decay rate. It is worth noticing in this context the work of Rashkovskiy, rooted in a classical electrodynamics framework in the length gauge.[38,39] This author proposed a nonlinear Schrödinger equation including a dissipative term depending on the third derivative of the dipole moment operator, that describes the inverse action of the self-radiation field on the electron wave consistently with the Abraham-Lorentz force.[39]

In parallel, the development of first-principles approaches hinging on time-dependent density functional theory (TDDFT) has expanded the scope and the realism of light-matter simulations at the molecular level.[40–44] The implementation of quantum-electrodynamical density-functional theory by Flick, Appel, Ruggenthaler, Rubio, Tokatly, and co-authors, has allowed for the examination of strongly coupled light-matter systems in cavities or in free-space including the quantum treatment of the light.[42,43,45,46] Recent studies in the frequency domain have applied these developments to describe collective excitations not only of electronic but also of vibrational states, and have addressed the emergence of polaritons and the possible modification of molecular properties via the quantum hybridization of light and mater.[47–50] On the other hand, in their real time treatment in the Coulomb Gauge,[44] Schäfer and Johanson arrived in three dimensions to the same potential as proposed by Rashkovskiy through a completely different path. This potential was implemented in a TDDFT scheme and

applied to describe, among other phenomena, the superradiance of Na dimers.[44] In one dimension, however, the potential derived by these authors predicts radiation from a free charge, provided its velocity has a component at right angles to the optical waveguide.

In recent work, starting from a mixed quantum-classical Lagrangian and the dipolar approximation, we developed an equation of motion for electron dynamics including energy dissipation from radiative emission which is able to reproduce, without the use of parameters, decay rates, absorption intensities and natural broadening in agreement with the Fermi golden rule.[51] This approach describes in the velocity gauge the same radiation field as the theory of Rashkovskiy in the lenght gauge.[52] In the Supporting Information we show that, same as that theory, it leads to the Abraham-Lorentz force, from which it can be expected that this treatment and those in references [39] and [44] produce comparable dynamics. Our equation of motion is also closely connected to the master equation introduced by Agarwall in his approach to spontaneous emission using a two level system[53] (see next section). The efficiency and versatility of our scheme allowed us to implement it in *ab initio* TDDFT simulations, in which context the model predicted the excited state lifetimes of atoms and ions with an accuracy within the experimental error.[51]

Similarly to other semiclassical approaches, this formalism does not include spontaneous emission from a stationary state,[54] meaning with this that the system will not relax from an eigenstate unless it is perturbed. This can lead to discrepancies with respect to the Fermi golden Rule at high temperatures or when the excited states are highly populated.[51,52] The role of the initial state is discussed in the Supporting Information. On the other hand, implicit in the derivation of the equation of motion is the long wave approximation, which assumes that the radiated field instantaneously affects the entire system, neglecting the retardation associated with the spatial separation. Nevertheless, at moderate electronic temperatures and subwavelength scales as those usually relevant in cooperative emission, such artifacts are assumed to have minor effects on the dynamics. In this communication we formally demonstrate that, for a collection of two level systems, our model predicts the super and subradiant effects consistently with Dicke's theory,[3] or with the Born-Markov approximation in the subwavelength limit.[2,55,56] Furthermore, we perform for the first time *ab initio* quantum dynamics simulations of cooperative emission in a molecular system, exploring the role of spatial distribution, molecular orientation, and applied field, on the coherent radiative response of a set of hydrogen molecules. In particular, we describe how the application of external fields can be employed to manipulate the subradiant states to store and release optical energy. Overall, our simulations provide the grounds to tailor collective radiation to optimize emission enhancement or supression in a molecular assembly.

First-principles electron dynamics were performed numerically at the TDDFT level with the LIO program, an open source DFT package developed and maintained by our group,[57] based on Gaussian basis functions and thoroughly optimized for parallel GPU computing.[58–60] The density matrix ρ was evolved according to the semiclassical dissipative equation of motion introduced in ref.[51] , including an acceleration factor. Details on the electronic structure calculations and on the evolution of the density matrix are given in the Supporting Information.

Collective emission in the dissipative model: formal derivation. The aim of what follows is to demonstrate that, for a collection of two-level systems, our semiclassical model reproduces the physics of cooperative emission in agreement with Dicke's formalism. The derived equations however are not employed in the TDDFT numerical simulations presented in the upcoming sections, which are instead directly based on the propagation of the dissipative equation of motion presented in ref.[51] (Eq. 1 of the Supporting Information).

In terms of the wavefunction $|\phi\rangle$, this equation reads:

$$|\dot{\phi}\rangle = -\frac{i}{\hbar}\tilde{H}|\phi\rangle \tag{1}$$

with the time dependent Hamiltonian $\tilde{H}$ defined to first order as:

$$\tilde{H} = \hat{H} + \frac{A}{\mathrm{i}\hbar}\langle\ddot{\mu}\rangle[\hat{\mu}, \hat{H}]. \tag{2}$$

Here $\hat{H}$ is the time-independent Hamiltonian, $\hat{\mu}$ the dipole moment operator ($\hat{\mu} = -e\sum_i \hat{r}_i$), and $A = \frac{\mu_0}{6\pi c}$. The quantity $\langle\ddot{\mu}\rangle$ is the mean value of the second time-derivative of the dipole moment, which can be approximated according to:[51]

$$\langle\ddot{\mu}\rangle = -\frac{1}{\hbar^2}\mathrm{Tr}\{\hat{\rho}[[\hat{\mu}, \hat{H}], \hat{H}]\} \tag{3}$$

where $\hat{\rho}$ is the density matrix, $\hat{\rho} = \sum_i |\phi_i\rangle\langle\phi_i|$. For the particular case of N identical non-interacting two level systems (TLS) as those considered by Dicke in his original work,[3] the Hamiltonian and the dipole moment operators can be represented as follows:

$$\hat{H} = \sum_{j=1}^{N} -\frac{\hbar\omega}{2}\hat{\sigma}_z^j\,, \tag{4}$$

$$\hat{\mu} = \sum_{j=1}^{N} \mu_{12}\hat{\sigma}_x^j\,, \tag{5}$$

where $\hbar\omega$ and μ_{12} are the excitation energy and the transition dipole moment for each TLS. $\hat{\sigma}_z^j$ and $\hat{\sigma}_x^j$ are Pauli operators acting on a single TLS j, where $[\hat{\sigma}_z^j, \hat{\sigma}_x^j] = 2\mathrm{i}\hat{\sigma}_y^j$. In this way we can rewrite Eqs. 2 and 3 in the following terms:

$$\tilde{H} = \sum_{j=1}^{N} -\frac{\hbar\omega}{2}\hat{\sigma}_z^j + A\mu_{12}\omega\langle\ddot{\mu}\rangle\hat{\sigma}_y^j,$$

$$\langle\ddot{\mu}\rangle = -\mu_{12}\omega^2\sum_{k=1}^{N}\mathrm{Tr}\left\{\rho^k\sigma_x^k\right\} = -\mu_{12}\omega^2\sum_{k=1}^{N}(\rho_{12}^k + \rho_{21}^k). \tag{6}$$

In the last equation we introduced ρ^k and σ_x^k as the matrix representation of the respective operators in the orthogonal basis of the eigenfuctions of the TLS, with ρ_{ij}^k the corresponding matrix elements. Thus, the evolution of the density matrix can be expressed independently for each TLS,

$$\frac{\partial\rho^j}{\partial t} = -\frac{\mathrm{i}}{\hbar}[\tilde{H}^j, \rho^j] \quad = \mathrm{i}\frac{\omega}{2}[\sigma_z^j, \rho^j] - \frac{\mathrm{i}}{\hbar}A\mu_{12}\omega\langle\ddot{\mu}\rangle[\sigma_y^j, \rho^j]\,, \tag{7}$$

where the only coupling between the N systems is mediated by the dipole moment through the second term on the right hand side. This term can be similarly identified in the equation of motion for the one-particle density matrix obtained on the basis of a different treatment by Agarwal,[53] which convalidates the present outcome. Assuming that the characteristic frequencies of the diagonal elements of ρ are much lower than those associated with the off-diagonal elements,

and averaging out the fast oscillations, insertion of Eq. 6 in the last expression eventually leads to:

$$\frac{\partial \rho_{11}}{\partial t} = -\frac{\partial \rho_{22}}{\partial t} = 2\gamma N \rho_{12}\rho_{21} = 2\gamma N \rho_{11}\rho_{22} \tag{8}$$

with $\gamma = \frac{A}{\hbar}\omega^3 \mu_{12}^2$ (see Supporting Information for a step by step derivation of this result). This formula can be employed to express the radiated power W,

$$W = \frac{\partial \langle H \rangle}{\partial t} = \frac{\partial}{\partial t}\mathrm{Tr}\{\rho H\} = 2\hbar\omega\gamma N^2 \rho_{11}\rho_{22}. \tag{9}$$

Dicke's theory is formulated in terms of the number of states in the ground and in the excited states, N_1 and N_2 respectively. Our formalism considers instead an ensemble of identical TLS with fractional occupations. The two treatments are connected through the relation $N_1 = \rho_{11}N$ and $N_2 = \rho_{22}N$, which gives

$$W = \frac{4}{3}\frac{\mu_{12}^2\omega^4}{c^3} N_2 N_1. \tag{10}$$

The radiated power in Dicke's formulation of superradiance is

$$W = \frac{4}{3}\frac{\mu_{12}^2\omega^4}{c^3} N_2(N_1+1) \tag{11}$$

with the prefactor $(4/3)\mu_{12}^2\omega^4/c^3$ being the energy dissipated per unit time by a single emitter. Hence, our semiclassical model predicts the quadratic dependence with respect to the number of molecules consistently with the quantum theory of superradiance, but for the fact that the factor $N_2(N_1+1)$ becomes N_2N_1. In the limit of large N_1, or equivalently, for the case of small excitations, both models converge to a same result. This coincidence is not surprising since, as we showed elsewhere,[51,52] small displacements from the ground state lead to better agreement with the Fermi golden rule. The additional term in Dicke's formulation is a consequence of spontaneous emission,[2] not present in our semiclassical scheme: when all the emitters are in the excited eigenstate, or $N_1 = 0$, the dissipated energy is zero because the system does not relax to the ground state.

To model subradiance, we consider two sets of non-interacting emitters, of sizes N_A and N_B respectively, with $N = N_A + N_B$. All TLS in both sets bear the same Hamiltonian and dipole moment operators, but evolve according to different density matrices ρ^A and ρ^B resulting from distinct excitations (e.g., only the molecules in set A are excited, all of them exposed to the same perturbation). In this scenario, the second derivative of the dipole (Eq. 6) now becomes

$$\langle \ddot{\mu} \rangle = -\mu_{12}\omega^2 \left[N_A(\rho_{12}^A + \rho_{21}^A) + N_B(\rho_{12}^B + \rho_{21}^B) \right] \tag{12}$$

and therefore the time derivative of the electronic populations can be written as:

$$\frac{1}{2\gamma}\frac{\partial \rho_{11}^A}{\partial t} =$$
$$= N_B\left(\mathbb{R}\{\rho_{21}^A\rho_{12}^B\} + \mathbb{R}\{\rho_{12}^A\rho_{12}^B\}\right) + N_A\left(\rho_{11}^A\rho_{22}^A + \mathbb{R}\{\rho_{12}^A\rho_{12}^A\}\right),$$
$$\frac{1}{2\gamma}\frac{\partial \rho_{11}^B}{\partial t} =$$
$$= N_A\left(\mathbb{R}\{\rho_{21}^A\rho_{12}^B\} + \mathbb{R}\{\rho_{12}^A\rho_{12}^B\}\right) + N_B\left(\rho_{11}^B\rho_{22}^B + \mathbb{R}\{\rho_{12}^B\rho_{12}^B\}\right). \tag{13}$$

where $\mathbb{R}$ denotes the real part. These equations, by contrast with the superradiant case (Eq. 11), admit a stationary solution different from the system eigenstates. It must satisfy

$$N_A^2\left[\rho_{11}^A\rho_{22}^A + \mathbb{R}\{\rho_{12}^A\rho_{12}^A\}\right] = N_B^2\left[\rho_{11}^B\rho_{22}^B + \mathbb{R}\{\rho_{12}^B\rho_{12}^B\}\right]. \tag{14}$$

To lowest order in the dissipation we have

$$\begin{aligned} \rho_{12}^A &= \sqrt{\rho_{11}^A\rho_{22}^A}\exp[i(\omega t - \phi_A)] \\ \rho_{12}^B &= \sqrt{\rho_{11}^B\rho_{22}^B}\exp[i(\omega t - \phi_B)]. \end{aligned} \tag{15}$$

In the stationary state, Eq. 13 requires that $\mathbb{R}\{\rho_{21}^A\rho_{12}^B\} + \mathbb{R}\{\rho_{12}^A\rho_{12}^B\} < 0$, otherwise the second term, always positive, could not be compensated by the first one. To satisfy this inequality $\mathbb{R}\{\rho_{12}^A\}$ and $\mathbb{R}\{\rho_{12}^B\}$ must bear different signs, which (from Eq. 15) implies:

$$\cos(\omega t - \phi_A) = -\cos(\omega t - \phi_B). \tag{16}$$

For this to hold, we find that $\phi_A = \phi_B \pm \pi$, meaning that in the subradiant regime subsets A and B evolve in counterphase. With the two coherences in antiphase, the balance condition in Eq. 14 reduces to $N_A^2\rho_{11}^A\rho_{22}^A = N_B^2\rho_{11}^B\rho_{22}^B$. This simply ensures that

$$N_A\rho_{12}^A = -N_B\rho_{12}^B \tag{17}$$

and that therefore $\langle \ddot{\mu} \rangle = 0$ with zero radiation. In such a stationary state the energy dissipation vanishes,

$$W = \frac{\partial \langle H \rangle}{\partial t} = \frac{\partial}{\partial t}\mathrm{Tr}\{\rho H\} = 2N_A\frac{\partial \rho_{11}^A}{\partial t} + 2N_B\frac{\partial \rho_{11}^B}{\partial t} = 0. \tag{18}$$

This result is further analyzed in the context of the molecular simulations presented below.

Superradiance in molecular arrays: the role of orientation and distance. For this exploratory approach we choose to examine a number of simple cases consisting of collections of H_2 molecules in different configurations. All the simulations discussed in what follows have been based on the propagation of equation Eq. 1 in a TDDFT framework, as specified in the Supporting Information. The first and more intense electronic transition in molecular hydrogen is predicted to be, depending on the basis set, between 83.45 nm and 109.7 nm within the present TDDFT level of theory, wavelengths falling far above the intermolecular separations considered in the models examined herein. The direction of the applied field is always parallel to the orientation of the H-H bond, which maximizes the light-matter coupling. Figure 1A shows the time evolution of the energy for different arrangements of hydrogen molecules upon illumination with a short pulse. Results corresponding to the accelerated form of the equation of motion are presented for a single H_2 molecule, and for ensembles of two, three and four molecules aligned in a row, with their internuclear axes laid parallel to each other and perpendicular to the intermolecular direction. The separation between monomers, of 10 Å, is large enough to render the interactions negligible, so that the only coupling is through the radiated electric field. It is seen that the deexcitation is speeded up as the size of the ensemble is increased. The logarithmic plots of the energy in the inset of Figure 1A show that for each model system the relaxation follows the expected exponential behavior. The dissipation rate, or equivalently the inverse of the radiative lifetime τ, can be obtained from the slope of each of these curves.[61] Figure 1B indicates that this rate grows proportionally to the number of molecules N, which means that the radiated power increases as N^2, in line with superradiant emission in

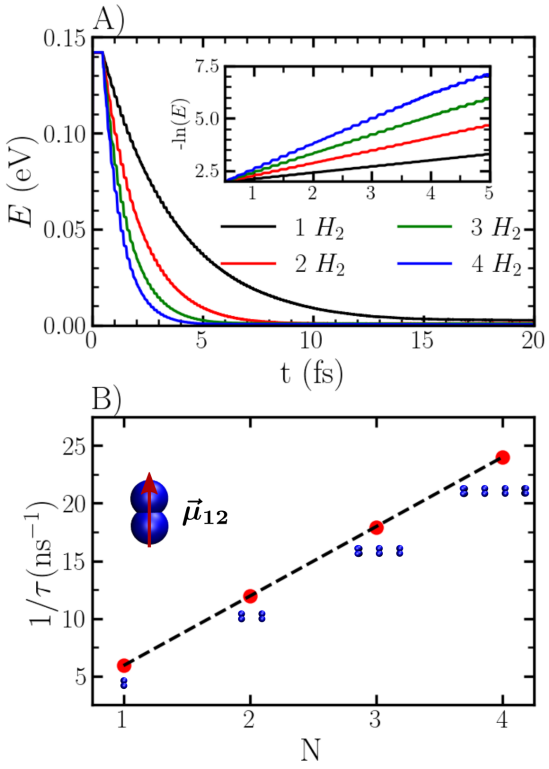

Figure 1. A) Temporal evolution of the electronic energy, relative to the ground state, for the relaxation of linear arrays of H_2 with different number of molecules. The distance between the monomers was 10 Å. In the inset, the logarithm of the energy is shown as a function of time. For the sake of comparison, the energies of the different systems are normalized by the number of molecules. B) Inverse of the radiative lifetime as a function of the number of molecules N.

the limit $N_1 \gg 1$.

To study the effect of intermolecular interactions on superradiance, simulations were performed on a chain of four H_2 molecules placed at different distances. For separations below 10 Å, the overlap between the molecular wavefunctions is not negligible and the use of diffuse basis proves to be important (see Supporting Information). Above these distances the molecules do not interact and the extension of the basis becomes irrelevant. Figure 2A presents the relaxation plots for this model system with the monomers oriented parallel to the intermolecular direction x. The simulations reveal that superradiance can be observed provided that the distance remains above 10 Å, being drastically deactivated at shorter separations. This quenching, sometimes called "van der Waals dephasing", is a consequence of the intermolecular interactions, represented here through the DFT potential. Since the environment is different for each molecule in the sample, these interactions break the symmetry of the system interfering with coherent emission, producing phase changes among the molecular states and finally damping superradiance.[2]

The quenching of the superradiance observed for the shorter separations can be avoided to some extent if the direction of the dipoles is chosen to be different from that relevant to the electromagnetic coupling arising in cooperative emission, i.e., if the two kinds of interactions are decoupled. This can be achieved by pointing the molecular dipoles perpendicularly to the x-axis. Figure 2B shows that in this configuration the system preserves the superradiance condition down to 8 Å, and even at shorter distances the relaxation exhibits some superradiant character.

The separation between individual emitters plays a critical part in the manifestation of superradiance in J-aggregates, where steric hindrance from functional groups or side chains tend to favor shorter radiative lifetimes.[24] In contrast, in densely packed molecular aggregates, the decoherence arising from van der Waals dephasing switches off the cooperative effects leading to slower decay rates. In those few experimental studies where the geometric patterns allowing for superradiant behavior have been characterized, intermolecular separations along the main axis have been found to be 7 Å or larger.[12,62] These lengths are in line with those encountered in our simulations.

Selective excitation: manipulation of subradiance. According to Dicke's work, when the applied field selectively affects part of the ensemble, exciting a number of molecules equal to N_x, the probability of emission will be equal to the excited fraction, N_x/N. If no photon is emitted, the excitation remains trapped in a dark-mode of the system as long as no further perturbation breaks in. This effect is called subradiance and arises as a consequence of the asymmetrical interaction of the molecular states, or a destructive interference mediated by the field. Ever since its discovery, this phenomenon has attracted much attention as a means to store optical energy. In the simulations considered so far, all the monomers were subject to the same excitation. In the present section we investigate the response upon excitation of a fraction of the system, using to this purpose the atomically localized potentials described in the methodological section.

Figure 3 displays the evolution of the energy following selective excitations of the monomers in a chain of four H_2 molecules distant 9 Å from each other, which is large enough to cut off any dispersive or electrostatic interactions. Ev-

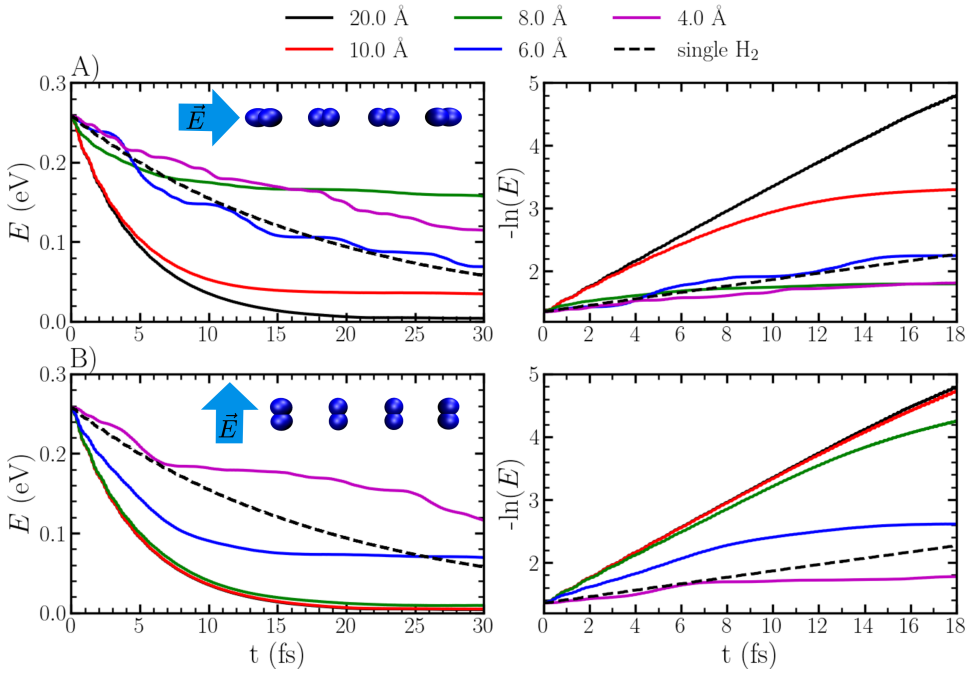

Figure 2. Temporal evolution of the electronic energy (left) and of its logarithm (right) for the relaxation of linear arrays of four H_2 monomers with different intermolecular separations, ranging from 1.5 to 10 Å. Panels (A) and (B) correspond, respectively, to molecular orientations parallel and perpendicular to the principal axis, as shown in the insets. The blue arrows point in the direction of the applied field. The dashed black line represents the decay of a single hydrogen molecule. The energy scale is relative to the ground state.

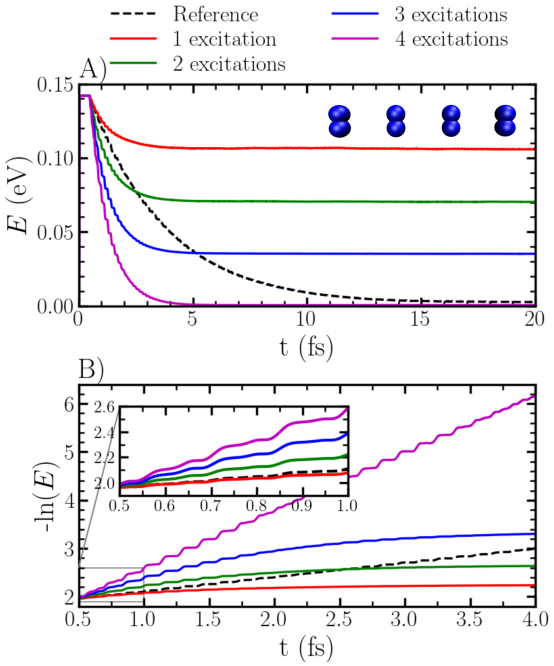

Figure 3. Temporal evolution of the electronic energy (A) and of its logarithm (B) for linear arrays of four H_2 monomers starting from the excitation of one, two, three or four molecules. The inset on panel B corresponds to the initial part of the dynamics. The dashed black line represents the decay of a single hydrogen molecule.

ery curve in the figure corresponds to the dynamics initiated after the coherent excitation of a different number of molecules, from one to four. In all four, the initial decay rate is accelerated with respect to the case of the isolated molecule. Eventually, however, the deexcitation ceases and the energy reaches a plateau above the ground state (with the exception of the superradiant system, shown in purple in Figure 3 and already discussed in the previous section). Remarkably, the energy dissipated in each case amounts to a fraction N_x/N of the total energy, where N_x is the number of molecules initially excited. In our density matrix representation, the evolution of the populations reflects the probabilities of finding the system in a given state. During the radiative decay, the probability of finding the system in the excited state decreases and then becomes constant. Thus, our simulations are reproducing the subradiant effect consistently with Dicke's quantum-mechanical formalism, predicting the end of radiative dissipation and the storage of optical energy in a dark state.

These results can be interpreted in the context of our semiclassical treatment through the examination of the time-dependent dipole moments of the sample and of the individual monomers. In particular, Figure 4 depicts this information following the excitation of a single monomer in the tetramer of molecular hydrogen. The molecule that is selectively excited develops an oscillatory dipole which, by radiative coupling, coherently stimulates the isoenergetic electronic transitions in the surrounding monomers. The charge density of the latter responds in counterphase to the induction, so that the dipolar fluctuations of the monomers tend to cancel with each other provoking the gradual declination of the total dipole moment (Figure 4A and 4B). Along this process the emitted and absorbed energies progressively equilibrate until a steady state is reached, in which all the molecules are partially excited. In this non-radiative steady state the charge densities of the individual molecules are

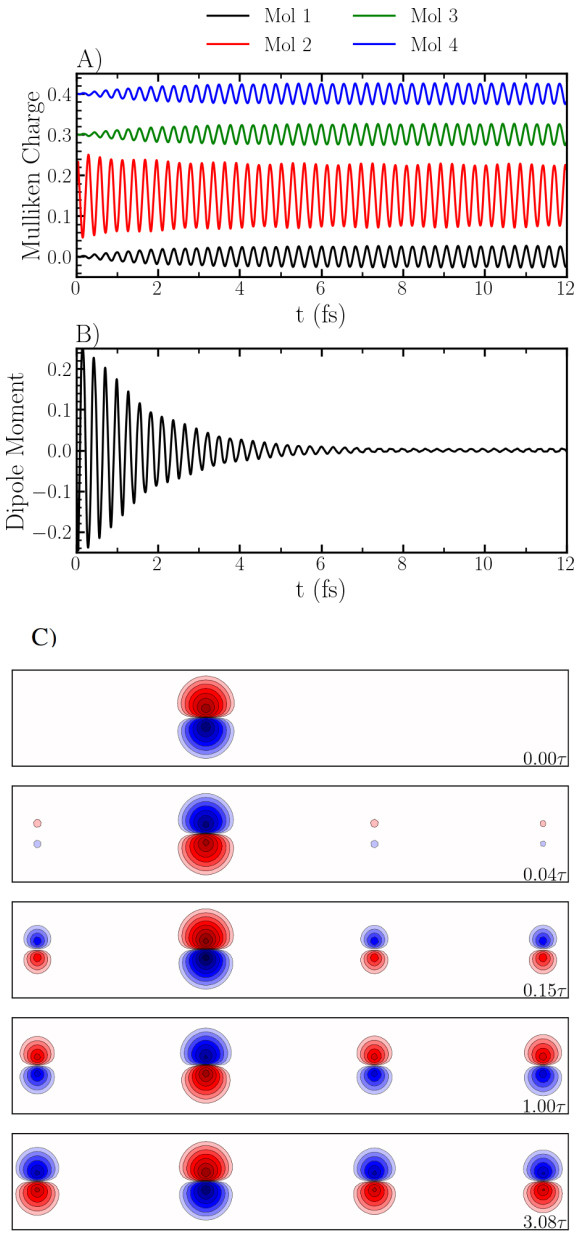

Figure 4. Temporal evolution of the atomic charges of the different molecules (A) and of the total dipole moment (B), for a linear array of four hydrogen molecules lying perpendicular to the intermolecular axis, upon the excitation of molecule 2. Magnitudes given in atomic units. (C) Sequence of contour plots displaying the density fluctuations for a subradiant chain of four H_2 molecules. Each panel corresponds to a different time along the dynamics, expressed in units of the radiative lifetime, and portrays the difference between the instantaneous electron density and that of the resting state. The excitation is applied at time zero on the second molecule from the left.

not at rest, but describe asymetric oscillations that mutually compensate each other yielding a vanishing variation of the net dipole moment, and therefore stopping the energy dissipation to the environment. Figure 4C provides a pictorial representation of this phenomenon in terms of the evolution of the electron densities.

Probably as important as the characterization of these non-emitting modes, it is the understanding of how to manipulate them, in particular of the ways in which the stored energy can be exchanged or released. With this purpose, we have investigated the effect of short light pulses on the evolution of the subradiant states once they have reached the stationary state. Two approaches were adopted for the application of this second pulse: the exposure of the entire sample to the same perturbation, or the excitation of a single, selected molecule. In the first kind of tests, the applied field is evenly absorbed by all the molecules resulting in increased amplitudes of the dipolar oscillations, but without causing any dephasing that led to a destabilization of the dark state. On the other hand, when just one molecule is targeted by the perturbation, a jump in the energy is observed followed by the resurgence of a net oscillatory dipole moment. These oscillations reactivate radiative dissipation, but with the individual dipoles of the monomers still fluctuating out of phase, so that eventually the system finds a new non-emitting mode above the ground state.

Importantly, the energetic jump occurring upon the application of the pulse to the subradiant state can be either positive or negative, depending on the timing of the perturbation. If it is positive, the transient that follows the excitation ends up in a dark state above the initial energy of the system. Conversely, if this jump is negative, the final state has a lower energy compared to the initial one. Figure 5 shows the temporal evolution of the dipole moment along with the total energy, for a simulation of the second kind, where the pulse produces a drop of the energy. After a dissipative transient the system reaches a new dark mode, so that the net outcome is a (partial) release of the optical energy trapped in the departing state.

What determines the sign and magnitude of the energetic jump induced by the second pulse is the relative alignment of the phase of the laser with respect to that of the molecular dipole that is being excited. When both are in phase, the pulse reinforces the dipolar fluctuations promoting the system to an excited state of higher energy. Instead, when the pulse is tuned to resonate in opposition to the direction of the dipole, the oscillations are damped and the overall process results in a net relaxation of the system. Indeed, with a sequence of pulses of the appropriate phase, the optical energy stored in a dark mode can thus be totally retrieved.

As it was shown in the superradiant limit, another factor that can be exploited to modulate cooperative emission is molecular orientation. To explore this variable, we considered a H_2 dimer in which each monomer was contained on a plane parallel to that of the other forming different dihedral angles θ, as illustrated on the inset of Figure 6A. Superradiant and subradiant states were simulated for different values of θ. To induce the superradiant regime both molecules were excited with the same pulse, while on the other hand a subradiant state emerged from a single excitation. The method of the localized potentials was employed. The results, depicted in Figure 6, show that collective emission is decoupled in both kind of phenomena as θ approaches 90^o, when the molecular axes become perpendicular to each other. In

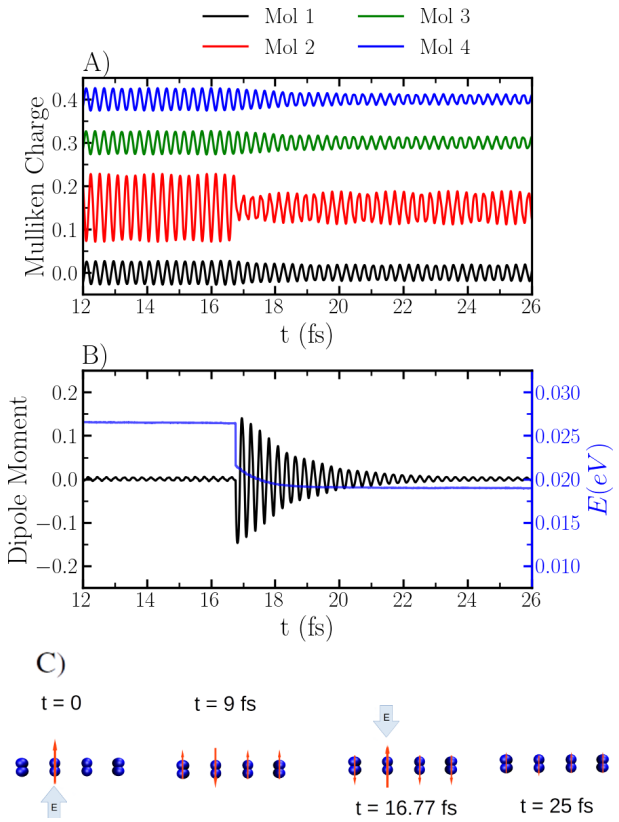

Figure 5. Temporal evolution of the atomic charges of the different molecules (A) and of the energy and total dipole moment (B), for a linear array of four hydrogen molecules in a subradiant stationary state (prepared from the excitation of molecule 2, Figure 4) that is perturbed with an electromagnetic pulse applied on molecule 2 at 16.77 fs. Charge and dipole moment expressed in atomic units. (C) Temporal sequence illustrating the application of the pulses and the direction of the instantaneous dipoles on every monomer at selected times.

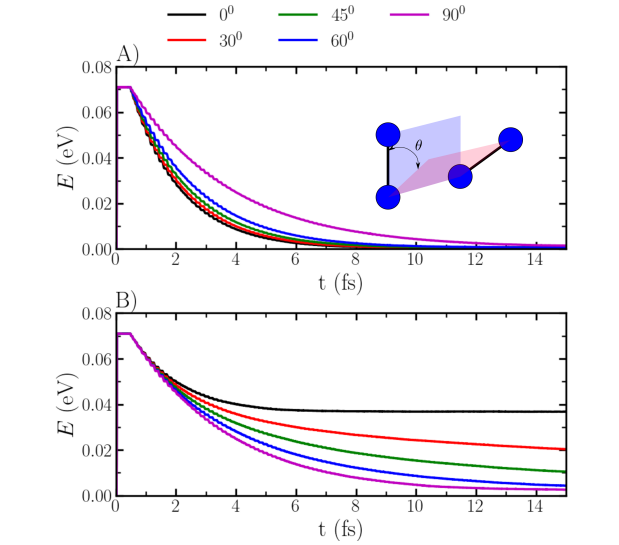

Figure 6. Temporal evolution of the electronic energy for a dimer of hydrogen molecules laying on parallel planes at different dihedral angles θ. A) Simultaneous excitation of both monomers: superradiance. B) Selective excitation of one of the monomers: subradiance. Energies relative to the ground state.

other words, the perpendicular alignment of the molecular dipoles prevents the interaction through the radiated field, and the relaxation reproduces the spontaneous emission of a single molecule (purple lines in Figure 6A and B). This effect is particularly attractive in the context of subradiant molecular arrays, where the rotation of the emitters can act as a switch to manage the release of photons. This would require a fine control of the molecular orientation, which may be challenging in the case of non-polar species as hydrogen, but that can be feasible with the adoption of polar monomers sensitive to external fields.

Summary. Combining TDDFT with a semiclassical formalism for radiative dissipation, this work examines the superradiance and subradiance of arrays of molecular hydrogen. First, it is proved that the semiclassical theory predicts both phenomena for sets of two-level systems. Then, the results from numerical dynamics on structures formed by up to four H_2 molecules are analyzed. In response to the simultaneous excitation of all the monomers, our simulations show a speedup in the emission rate associated with a decrease of the radiative lifetime linear with the number of molecules, which is the signature of superradiance. This behavior exhibits a strong dependence on distance and orientation. When the molecular dipoles are aligned with the main axis of the array, i.e., the one parallel to the electromagnetic interaction, a fast decoherence that kills the superradiant emission manifests for intermolecular distances below 10 Å. These distances can be substantially reduced if the dipoles are rotated perpendicularly to this axis. In this configuration the superradiance regime is preserved down to separations comparable to the length of a covalent bond, for which the H_2 monomers start to loose their individual identities.

The selective excitation of only part of the sample leads to a subradiant state where the dipole moments of the H_2 monomers develop out of phase oscillations that compensate with each other cancelling any net energy dissipation. The orientation of the dipoles determines the electromagnetic coupling and therefore the subradiant character of the sample. The application of a second laser pulse on a subset of molecules may be used to tune the energy of the subradiant system, which can reversibly absorb or emit radiation depending on the phase of the incident field. A sequence of pulses can be employed for a complete withdrawal of the electromagnetic energy while returning the system to its ground state. Through the calibration of the phase, amplitude and duration of the perturbation, it might be possible to drive the system from a subradiant to a superradiant state and release the entire "load" of optical energy with a single pulse.

This study contributes fundamental and quantitative insights for the manipulation of light based on cooperative emission of molecules. Importantly, it provides a basis for subradiant energy storage by the fine-tuning of laser pulses. Furthermore, it suggests that superradiance and subradiance can be enhanced through the construction of dense molecular chains, where the separation between the monomers can be minimized below the limit imposed by the van der Waals interactions, provided that their dipoles point in the proper direction. The adoption of polar monomers introduces the possibility of controlling the molecular alignment via an external potential, that could be used to switch on and off collective emission. These simulations are the first to describe the time-dependent cooperative radiation of realistic models of molecular assemblies. The mergence of dissipative dynamics with real-time TDDFT and atomically localized po-

tentials proved successful in addressing the time-dependent cooperative radiation of realistic models of molecular assemblies. The present approach constitutes a unique framework to understand, design and optimize superradiant and subradiant architectures based on tridimensional molecular arrays.

Supporting Information

Methodological details on the TDDFT simulations and on the excitation schemes (Gaussian and laser pulses), discussion on the role of the initial state in the dynamics, and auxiliary derivations.

Acknowledgements

This work has been funded by the European Union's Horizon 2020 research and innovation programme through the project ATLANTIC under grant agreement No 823897. We acknowledge Agencia Nacional de Promoción Científica y Tecnológica de Argentina (PICT 2020-02804 and PICT 2016-3167).

References

(1) Scully, M. O.; Svidzinsky, A. A. The super of superradiance. *Science* **2009**, *325*, 1510–1511.
(2) Gross, M.; Haroche, S. Superradiance: An essay on the theory of collective spontaneous emission. *Phys. Rep.* **1982**, *93*, 301–396.
(3) Dicke, R. H. Coherence in spontaneous radiation processes. *Phys. Rev.* **1954**, *93*, 99.
(4) Skribanowitz, N.; Herman, I. P.; MacGillivray, J. C.; Feld, M. S. Observation of Dicke Superradiance in Optically Pumped HF Gas. *Phys. Rev. Lett.* **1973**, *30*, 309–312.
(5) Crubellier, A.; Liberman, S.; Pillet, P. Doppler-Free Superradiance Experiments with Rb Atoms: Polarization Characteristics. *Phys. Rev. Lett.* **1978**, *41*, 1237–1240.
(6) Gross, M.; Fabre, C.; Pillet, P.; Haroche, S. Observation of Near-Infrared Dicke Superradiance on Cascading Transitions in Atomic Sodium. *Phys. Rev. Lett.* **1976**, *36*, 1035–1038.
(7) Vrehen, Q. H. F.; Hikspoors, H. M. J.; Gibbs, H. M. Quantum Beats in Superfluorescence in Atomic Cesium. *Phys. Rev. Lett.* **1977**, *38*, 764–767.
(8) DeVoe, R.; Brewer, R. Observation of superradiant and subradiant spontaneous emission of two trapped ions. *Phys. Rev. Lett.* **1996**, *76*, 2049.
(9) Bopp, M. A.; Jia, Y.; Li, L.; Cogdell, R. J.; Hochstrasser, R. M. Fluorescence and photobleaching dynamics of single light-harvesting complexes. *P. Natl. Acad. Sci. USA* **1997**, *94*, 10630–10635.
(10) Hettich, C.; Schmitt, C.; Zitzmann, J.; Kühn, S.; Gerhardt, I.; Sandoghdar, V. Nanometer resolution and coherent optical dipole coupling of two individual molecules. *Science* **2002**, *298*, 385–389.
(11) Scheibner, M.; Schmidt, T.; Worschech, L.; Forchel, A.; Bacher, G.; Passow, T.; Hommel, D. Superradiance of quantum dots. *Nature Phys.* **2007**, *3*, 106–110.
(12) Zhang, Y.; Luo, Y.; Zhang, Y.; Yu, Y.-J.; Kuang, Y.-M.; Zhang, L.; Meng, Q.-S.; Luo, Y.; Hou, J.-L. Y. Z.-C. D. J. G. Visualizing coherent intermolecular dipole–dipole coupling in real space. *Nature* **2016**, *531*, 623–627.
(13) Araújo, M. O.; Krešić, I.; Kaiser, R.; Guerin, W. Superradiance in a large and dilute cloud of cold atoms in the linear-optics regime. *Phys. Rev. Lett.* **2016**, *117*, 073002.
(14) Solano, P.; Barberis-Blostein, P.; Fatemi, F. K.; Orozco, L. A.; Rolston, S. L. Super-radiance reveals infinite-range dipole interactions through a nanofiber. *Nature Commun.* **2017**, *8*, 1–7.
(15) Rainò, G.; Becker, M. A.; Bodnarchuk, M. I.; Mahrt, R. F.; Kovalenko, M. V.; Stöferle, T. Superfluorescence from lead halide perovskite quantum dot superlattices. *Nature* **2018**, *563*, 671–676.
(16) Manna, B.; Nandi, A. Manifestation of unforeseen superradiance phenomenon from phenanthrene and chrysene nanoaggregates. *J. Phys. Chem. C* **2019**, *123*, 21281–21289.
(17) Luo, Y.; Chen, G.; Zhang, Y.; Zhang, L.; Yu, Y.; Kong, F.; Tian, X.; Zhang, Y.; Shan, C.; Luo, Y.; Yang, J.; Sandoghdar, V.; Dong, Z.; Hou, J. G. Electrically Driven Single-Photon Superradiance from Molecular Chains in a Plasmonic Nanocavity. *Phys. Rev. Lett.* **2019**, *122*, 233901.
(18) Pavolini, D.; Crubellier, A.; Pillet, P.; Cabaret, L.; Liberman, S. Experimental evidence for subradiance. *Phys. Rev. Lett.* **1985**, *54*, 1917.
(19) Takasu, Y.; Saito, Y.; Takahashi, Y.; Borkowski, M.; Ciuryło, R.; Julienne, P. S. Controlled production of subradiant states of a diatomic molecule in an optical lattice. *Phys. Rev. Lett.* **2012**, *108*, 173002.
(20) Guerin, W.; Araújo, M. O.; Kaiser, R. Subradiance in a Large Cloud of Cold Atoms. *Phys. Rev. Lett.* **2016**, *116*, 083601.
(21) Ferioli, G.; Glicenstein, A.; Henriet, L.; Ferrier-Barbut, I.; Browaeys, A. Storage and release of subradiant excitations in a dense atomic cloud. *Phys. Rev. X* **2021**, *11*, 021031.
(22) Spano, F. C.; Mukamel, S. Superradiance in molecular aggregates. *J. Chem. Phys.* **1989**, *91*, 683–700.
(23) Zhao, Y.; Meier, T.; Zhang, W. M.; Chernyak, V.; Mukamel, S. Superradiance Coherence Sizes in Single-Molecule Spectroscopy of LH2 Antenna Complexes. *J. Phys. Chem. B* **1999**, *103*, 3954–3962.
(24) Zhao, Y.; Wang, V.; Javey, A. Molecular Materials with Short Radiative Lifetime for High-Speed Light-Emitting Devices. *Matter* **2020**, *3*, 1832–1844.
(25) Bohnet, J. G.; Chen, Z.; Weiner, J. M.; Meiser, D.; Holland, M. J.; Thompson, J. K. A steady-state superradiant laser with less than one intracavity photon. *Nature* **2012**, *484*, 78–81.
(26) Iida, T. Control of Plasmonic Superradiance in Metallic Nanoparticle Assembly by Light-Induced Force and Fluctuations. *J. Phys. Chem. Lett.* **2012**, *3*, 332–336.
(27) Phuong, L.; Miyajima, K.; Maeno, K.; Itoh, T.; Ashida, M. Transitions from spontaneous emission to stimulated emission and superfluorescence of biexcitons confined in CuCl quantum dots. *J. Lumin.* **2013**, *133*, 77–80.
(28) Filipp, S.; Van Loo, A.; Baur, M.; Steffen, L.; Wallraff, A. Preparation of subradiant states using local qubit control in circuit QED. *Phys. Rev. A* **2011**, *84*, 061805.
(29) Holmes, J.; Sushma, A. A.; Tsvetkova, I. B.; Schaich, W. L.; Schaller, R. D.; Dragnea, B. Ultrafast Collective Excited-State Dynamics of a Virus-Supported Fluorophore Antenna. *J. Phys. Chem. Lett.* **2022**, *13*, 3237–3243.
(30) Asenjo-Garcia, A.; Moreno-Cardoner, M.; Albrecht, A.; Kimble, H.; Chang, D. E. Exponential improvement in photon storage fidelities using subradiance and "selective radiance" in atomic arrays. *Phys. Rev. X* **2017**, *7*, 031024.
(31) Facchinetti, G.; Jenkins, S. D.; Ruostekoski, J. Storing light with subradiant correlations in arrays of atoms. *Phys. Rev. Lett.* **2016**, *117*, 243601.
(32) Wild, D. S.; Shahmoon, E.; Yelin, S. F.; Lukin, M. D. Quantum nonlinear optics in atomically thin materials. *Phys. Rev. Lett.* **2018**, *121*, 123606.
(33) Guimond, P.-O.; Grankin, A.; Vasilyev, D.; Vermersch, B.; Zoller, P. Subradiant Bell states in distant atomic arrays. *Phys. Rev. Lett.* **2019**, *122*, 093601.
(34) Kimble, H. J. The quantum internet. *Nature* **2008**, *453*, 1023–1030.
(35) do Espirito Santo, T.; Weiss, P.; Cipris, A.; Kaiser, R.; Guerin, W.; Bachelard, R.; Schachenmayer, J. Collective excitation dynamics of a cold atom cloud. *Phys. Rev. A* **2020**, *101*, 013617.
(36) Betzholz, R.; Taketani, B. G.; Torres, J. M. Breakdown signatures of the phenomenological Lindblad master equation in the strong optomechanical coupling regime. *Quantum Sci. Technol.* **2021**, *6*, 015005.
(37) Jeske, J.; Ing, D. J.; Plenio, M. B.; Huelga, S. F.; Cole, J. H. Superradiance in molecular aggregates. *J. Chem. Phys.* **2015**, *142*, 064104.
(38) Rashkovskiy, S. A. Classical-field model of the hydrogen atom. *Indian J. Phys.* **2017**, *91*, 607–621.
(39) Rashkovskiy, S. A. Nonlinear Schrödinger equation and classical-field description of thermal radiation. *Indian J. Phys.* **2018**, *92*, 289–302.
(40) Tokatly, I. V. Time-Dependent Density Functional Theory for Many-Electron Systems Interacting with Cavity Photons. *Phys. Rev. Lett.* **2013**, *110*, 233001.
(41) Svendsen, M. K.; Kurman, Y.; Schmidt, P.; Koppens, F.; Kaminer, I.; Thygesen, K. S. Combining density functional theory with macroscopic QED for quantum light-matter interactions in 2D materials. *Nature Commun.* **2021**, *12*, 2778.
(42) Flick, J.; Ruggenthaler, M.; Appel, H.; Rubio, A. Kohn-Sham approach to quantum electrodynamical density-functional theory: Exact time-dependent effective potentials in real space. *Proc Natl Acad Sci USA* **2015**, *112*, 15285–15290.
(43) Ruggenthaler, M.; Tancogne-Dejean, N.; Flick, J.; Appel, H.; Rubio, A. From a quantum-electrodynamical light-matter description to novel spectroscopies. *Nat. Rev. Chem.* **2018**, *2*, 1–16.
(44) Schäfer, C.; Johansson, G. Shortcut to Self-Consistent Light-Matter Interaction and Realistic Spectra from First Principles. *Phys. Rev. Lett.* **2022**, *128*, 156402.
(45) Ruggenthaler, M.; Flick, J.; Pellegrini, C.; Appel, H.; Tokatly, I. V.; Rubio, A. Quantum-electrodynamical density-functional theory: Bridging quantum optics and electronic-structure theory. *Phys. Rev. A* **2014**, *90*, 012508.
(46) Pellegrini, C.; Flick, J.; Tokatly, I. V.; Appel, H.; Rubio, A. Optimized Effective Potential for Quantum Electrodynamical Time-Dependent Density Functional Theory. *Phys. Rev. Lett.* **2015**, *115*, 093001.
(47) Bonini, J.; Flick, J. Ab Initio Linear-Response Approach to Vibro-Polaritons in the Cavity Born-Oppenheimer Approximation. *J. Chem. Theory Comput.* **2022**, *18*, 2764–2773.
(48) Flick, J.; Ruggenthaler, M.; Appel, H.; Rubio, A. Atoms and molecules in cavities, from weak to strong coupling in quantum-electrodynamics (QED) chemistry. *Proc Natl Acad Sci USA* **2017**, *114*, 3026–3034.
(49) Flick, J.; Welakuh, D. M.; Ruggenthaler, M.; Appel, H.; Rubio, A. Light-Matter Response in Nonrelativistic Quantum Elec-

trodynamics. *ACS Photonics* **2019**, *6*, 2757–2778.
(50) Sidler, D.; Schäfer, C.; Ruggenthaler, M.; Rubio, A. Polaritonic Chemistry: Collective Strong Coupling Implies Strong Local Modification of Chemical Properties. *J. Phys. Chem. Lett.* **2021**, *12*, 508–516.
(51) Bustamante, C. M.; Gadea, E. D.; Horsfield, A.; Todorov, T. N.; Lebrero, M. C. G.; Scherlis, D. A. Dissipative equation of motion for electromagnetic radiation in quantum dynamics. *Phys. Rev. Lett.* **2021**, *126*, 087401.
(52) Gadea, E. D.; Bustamante, C. M.; Todorov, T. N.; Scherlis, D. A. Radiative thermalization in semiclassical simulations of light-matter interaction. *Phys. Rev. A* **2022**, *105*, 042201.
(53) Agarwal, G. S. Master-Equation Approach to Spontaneous Emission. III. Many-Body Aspects of Emission from Two-Level Atoms and the Effect of Inhomogeneous Broadening. *Phys. Rev. A* **1971**, *4*, 1791.
(54) Li, T. E.; Chen, H.-T.; Subotnik, J. E. Comparison of Different Classical, Semiclassical, and Quantum Treatments of Light–Matter Interactions: Understanding Energy Conservation. *J. Chem. Theory Comput.* **2019**, *15*, 1957–1973.
(55) Coffey, B.; Friedberg, R. Effect of short-range coulomb interaction on cooperative spontaneous emission. *Phys. Rev. A* **1978**, *17*, 1033.
(56) Agarwal, G. S. *Quantum Optics*; Springer, 1974; pp 1–128.
(57) The LIO Project. `https://github.com/MALBECC/LIO`, 2016.
(58) Nitsche, M. A.; Ferreria, M.; Mocskos, E. E.; Lebrero, M. C. G. A GPU accelerated implementation of DFT for hybrid QM/MM simulations. *J. Chem. Theory Comput.* **2014**, *10*, 959.
(59) Marcolongo, J. P.; Zeida, A.; Semelak, J. A.; Foglia, N. O.; Morzan, U. N.; Estrin, D. A.; González Lebrero, M. C.; Scherlis, D. A. Chemical Reactivity and Spectroscopy Explored From QM/MM Molecular Dynamics Simulations Using the LIO Code. *Front. Chem.* **2018**, *6*, 70.
(60) Morzan, U. N.; Ramírez, F. F.; Oviedo, M. B.; Sánchez, C. G.; Scherlis, D. A.; Gonzalez Lebrero, M. C. Electron dynamics in complex environments with real-time time dependent density functional theory in a QM-MM framework. *J. Chem. Phys.* **2014**, *140*.
(61) All simulations in this work were performed in the presence of an acceleration factor f in the dissipative term (eq. 1 in the SI). As a consequence, the time-scales in all Figures are significantly shorter than the characteristic molecular relaxation times. However, the radiative lifetimes in Figure 1B have been extrapolated to f=1 and therefore correspond to the physical lifetimes in the picosecond or nanosecond scale.
(62) Busse, G.; Frederichs, B.; Petrov, N. K.; Techert, S. Structure determination of thiacyanine dye J-aggregates in thin films: Comparison between spectroscopy and wide angle X-ray scattering. *Phys. Chem. Chem. Phys.* **2004**, *6*, 3309–3314.

TOC Graphic